J. Am. Chem. Soc. **1990**, *112*, 2083-2088

Ion Beam Studies of the Reaction of $Si^+(^2P)$ with Methane. Reaction Mechanisms and Thermochemistry of $SiCH_x^+$ (x = 1-3)

B. H. Boo,[†] J. L. Elkind,[‡] and P. B. Armentrout*[,§]

Contribution from the Departments of Chemistry, Chungnam National University, Daejeon 302-764, Korea, University of California, Berkeley, California 94720, and University of Utah, Salt Lake City, Utah 84112. *Received August 21, 1989*

Abstract: Guided ion beam mass spectrometry is used to examine the reaction of ground-state silicon ion with methane. Absolute cross sections of all products are measured from near-thermal to 14-eV relative kinetic energy. Only endothermic processes are observed with SiH^+ and SiH_3C^+ as the major ionic products. There is evidence that the latter species has two forms, $Si^+–CH_3$ formed at low energies and a higher energy form that could be a triplet state of $SiCH_3^+$ or $HSiCH_2^+$. Minor ionic products include $SiCH_2^+$, CH_3^+, and $SiCH^+$. The former product can be formed via the concomitant formation of molecular hydrogen or two hydrogen atoms. The latter process is much more efficient. All observed products are consistent with a reaction that occurs via an $HSiCH_3^+$ intermediate. From the measured thresholds of the reactions and other information, the 298 K heats of formation (kcal/mol) for the following silicon species are derived: $\Delta_f H°(SiH) = 91.4 \pm 1.8$, $\Delta_f H°(SiCH^+) = 339 \pm 7$, $\Delta_f H°(SiCH_2^+) = 285 \pm 3$, and $\Delta_f H°(SiCH_3^+) = 235 \pm 5$.

The activation of C–H bonds by silicon species is thought to be a pivotal process in understanding heterogeneous and homogeneous C–H activations, as well as for examining thermochemical properties of organosilicon species. C–H activations by a divalent silicon, silylene, have recently been the subject of a number of experimental[1-5] and theoretical[6,7] investigations. C–H activations by the divalent silicon center of silylenes usually occur intramolecularly due primarily to the large activation energy for these processes.[5,6] Intermolecular C–H insertion by silylenes is generally reserved for the studies of theoretical chemists.[6]

The reaction of atomic silicon ion with methane is an ideal system for examining inter- and intramolecular C–H activations by reactive silicon species, as well as determining the thermochemistry of organosilicon species. In the present study, we make a detailed investigation of the reaction of ground-state silicon ion (^2P) with methane using the guided ion beam technique. As studied by ion cyclotron resonance mass spectrometry,[8] silicon ions are not observed to react with methane at thermal energies, a result similar to the reactions of methane with almost all the atomic transition-metal ions.[9-11] However, translational energy can drive a variety of endothermic processes, which can all be explained via a simple reaction mechanism. Indeed, Cheng et al. have reported the formation of $SiCH_3^+$ and $SiCH_2^+$ in this system at elevated kinetic energies, although excited-state ions made an unknown contribution to this observation.[12] In the present work, quantitative studies of the translational energy dependence of the cross sections enable us to extract thermochemical data for SiH and $SiCH_x^+$ (x = 1-3) species.

Experimental Section

The guided ion beam apparatus has been described in detail previously.[13] Ground-state silicon ions (^2P) are produced by surface ionization of silane in which SiH_4 is exposed to a rhenium filament resistively heated to $\approx$2200 K.[14] Decomposition and ionization follow such that atomic silicon ions but no molecular ions are produced. Because the first excited state of Si^+ is 5.46 eV higher in energy than the ground state,[15] this source produces exclusively ground-state $Si^+(^2P)$. These ions are extracted from the ion source and focused into a magnetic momentum analyzer where the $^{28}Si^+$ isotope is selected. These ions are decelerated to a desired kinetic energy with an exponential retarding lens and focused into an octopole ion trap. Radio frequency electric fields applied to the octopole create a radial potential well in which ions are trapped over a broad mass range. The octopole passes through a gas cell filled with the reactant neutral gas. The pressure of the neutral gas is kept sufficiently low that single-collision conditions prevail. The product and unreacted ions are extracted from the octopole and injected into a quadrupole mass filter for mass analysis. Then, the ions are detected with a scintillation ion detector, and the signal is processed by standard ion pulse-counting techniques. Ion intensities are converted to absolute reaction cross sections as described previously.[13] Absolute and relative cross sections are estimated to have uncertainties of ±20% and ±5%, respectively.

Laboratory ion energies are converted to energies in the center of mass (CM) frame with the conversion $E(\mathrm{CM}) = E(\mathrm{lab})M/(m + M)$ where m and M are the masses of the projectile ion and target gas, respectively. The absolute zero of the energy scale and the distribution of ion energies are determined with the octopole as a retarding energy analyzer. This procedure is detailed elsewhere.[13] We estimate that the uncertainty in the ion energy scale is ±0.05-eV laboratory (±0.02-eV CM). The spread in the ion beam energy has a fwhm of 0.5 eV in the laboratory frame (~0.2-eV CM).

We have found from previous studies that the model excitation function

$$\sigma = \sigma_0(E - E_0)^n/E^m \qquad (1)$$

can accurately reproduce experimental cross sections in the threshold region. In this equation, σ_0 is an energy-independent scaling factor, E is the relative translational energy, E_0 is the endothermicity of the re-

---

[†] Chungnam National University.

[‡] University of California. Present address: Texas Instruments, Dallas, TX 75265.

[§] University of Utah. NSF Presidential Young Investigator 1984-1989; Alfred P. Sloan Fellow; Camille and Henry Dreyfus Teacher-Scholar, 1987-1992.

(1) Gaspar, P. P. *React. Intermed.* (*Wiley*) **1978**, *1*, 229; **1981**, *2*, 335; **1985**, *3*, 333.

(2) Sawrey, B. A.; O'Ring, H. E.; Ring, M. A.; Coffey, D. *Int. J. Chem. Kinet.* **1984**, *16*, 31.

(3) Davidson, I. M. T.; Ijadi-Maghsoodi, S.; Barton, T. J.; Tillman, N. *J. Chem. Soc., Chem. Commun.* **1984**, 478.

(4) Wulffe, W. D.; Goure, W. F.; Barton, T. J. *J. Am. Chem. Soc.* **1978**, *100*, 6328.

(5) Boo, B. H.; Gaspar, P. P. *Organometallics* **1986**, *5*, 698.

(6) Gordon, M. S.; Gano, D. R. *J. Am. Chem. Soc.* **1984**, *106*, 5421.

(7) Nagase, S.; Kudo, T. *J. Chem. Soc., Chem. Commun.* **1984**, 141.

(8) Stewart, G. W.; Henis, J. M. S.; Gaspar, P. P. *J. Chem. Phys.* **1972**, *57*, 1990.

(9) Aristov, N.; Armentrout, P. B. *J. Phys. Chem.* **1987**, *91*, 6178. Schultz, R. H.; Elkind, J. L.; Armentrout, P. B. *J. Am. Chem. Soc.* **1988**, *110*, 411. Sunderlin, L. S.; Armentrout, P. B. *J. Phys. Chem.* **1988**, *92*, 1209. Georgiadis, R.; Armentrout, P. B. *J. Phys. Chem.* **1988**, *92*, 7067. Sunderlin, L. S.; Armentrout, P. B. *J. Am. Chem. Soc.* **1989**, *111*, 3845.

(10) Armentrout, P. B.; Beauchamp, J. L. *J. Am. Chem. Soc.* **1981**, *103*, 784.

(11) Byrd, G. D.; Freiser, B. S. *J. Am. Chem. Soc.* **1982**, *104*, 5944. Wise, M. B.; Jacobson, D. B.; Freiser, B. S. *J. Am. Chem. Soc.* **1985**, *107*, 1590, 6744.

(12) Cheng, T. M. H.; Yu, T.-Y.; Lampe, F. W. *J. Phys. Chem.* **1973**, *77*, 2587.

(13) Ervin, K. M.; Armentrout, P. B. *J. Phys. Chem.* **1985**, *83*, 166.

(14) Boo, B. H.; Armentrout, P. B. *J. Am. Chem. Soc.* **1987**, *109*, 3549.

(15) Moore, C. E. *Natl. Stand. Ref. Data Ser.*, (*U.S. Natl. Bur. Stand.*) **1970**, *34*.

0002-7863/90/1512-2083$02.50/0

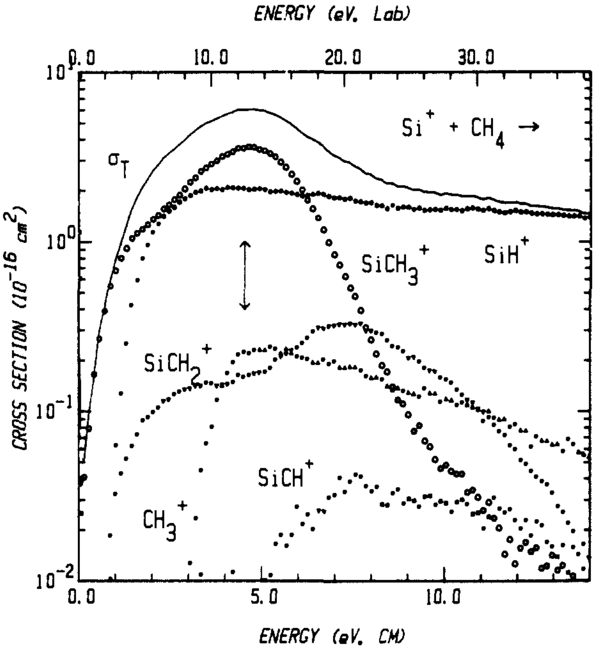

Figure 1. Variation of product cross sections with translational energy in the laboratory frame (upper scale) and the center-of-mass energy frame (lower scale) for the reaction of Si^+ with CH_4. The line shows the total cross section for all products.

action, and *n* and *m* are variable parameters. The excitation function with $m = 1$ is among the most useful for translationally driven reactions[16] and is fouund to be quite accurate in deriving reaction thresholds.[9,14,17-20] Values for E_0 are determined by convoluting the model cross section with the known kinetic energy distributions, comparing this to the data, and then optimizing the parameters in eq 1 with nonlinear least-squares methods.

As the relative kinetic energy is increased, reaction cross sections typically reach maxima and then decline due to product dissociation or to competition with other product channels. We have modeled the energy dependence of this high-energy part of the cross section by using eq 2,

$$\sigma = \sigma_0(E - E_0)^n(1 - P_D)/E^m \qquad (2)$$

where P_D is the probability of product dissociation.[21] P_D is controlled by two parameters: *p*, which is an adjustable parameter, and E_D, which is the energy at which product ions begin decomposing; i.e., $P_D = 0$ for $E < E_D$.

Silane with semiconductor purity was purchased from Matheson Co. Deuteriated methane was purchased from MSD Isotopes Co.

Results

Results for the reaction of Si^+ with CH_4 are shown in Figure 1. Similar results were also obtained for reaction with CD_4. The lowest energy process is formation of an ionic product corresponding to SiH_3C^+ as in reaction 3. This cross section displays

$$Si^+ + CH_4 \rightarrow SiH_3C^+ + H \qquad (3)$$

an odd shape and a reproducible break at around 2 eV (also shown in Figure 2). Possible explanations for this unusual behavior will be discussed further below. The cross section for SiH_3C^+ begins to decline at about 4.5 eV. This suggests that the primary dissociation patthway for SiH_3C^+ is loss of CH_3, the overall process (4). This reaction has a thermodynamic threshold of $D°(H-CH_3)$ = 4.54 eV.

$$Si^+ + CH_4 \rightarrow Si^+ + CH_3 + H \qquad (4)$$

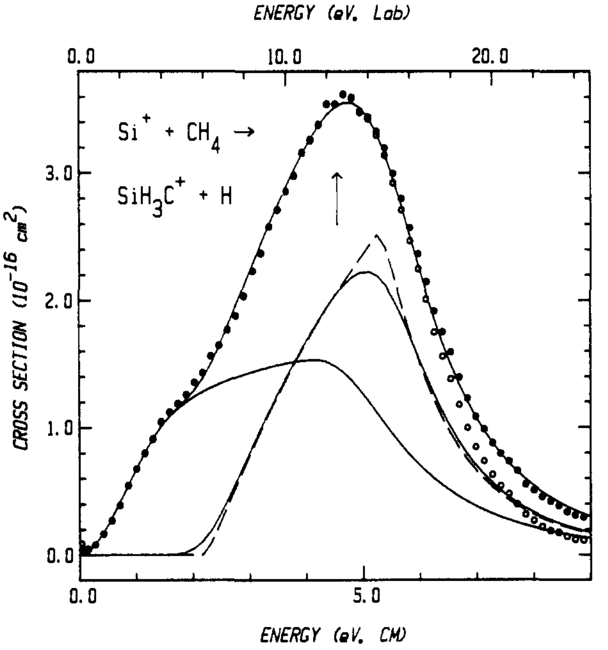

Figure 2. Cross section for SiH_3C^+ formed in the reaction of Si^+ with CH_4 as a function of the translational energy in the laboratory frame (upper scale) and the center-of-mass frame (lower scale). The experimental data for SiH_3C^+ (open circles) are compared with model cross sections at low and high energies and their sum as described in the text and Table III. The full lines show the models convoluted over the experimental energy distribution, and the broken line shows the high-energy unconvoluted fit. The arrow indicates $D°(H-CH_3)$ at 4.54 eV. Closed circles show the sum of the cross sections for SiH_3C^+ and $SiCH_2^+$ + 2H (the latter is shown in Figure 4).

Table I. Heats of Formation (kcal/mol) at 298 K[a]

species	$\Delta_fH°$	species	$\Delta_fH°$
H	52.1	C_2H_4	12.5 (0.1)
CH	142.0 (4.2)	C_2H_6	-20.0 (0.1)[b]
CH_2	92.35 (1.0)	CH_3^+	263.2 (0.5)[c]
CH_3	34.8 (0.2)	Si^+	297.1 (1)
CH_4	-17.9 (0.1)	H_3SiCH_3	-6.9 (1)[d]
C_2H_2	54.2 (0.2)	$HSi(CH_3)_3$	-39.0 (1)[d]
		$Si(CH_3)_4$	-54.1 (1.1),[e] -55.4[d]

[a] Values are from ref 34 unless noted otherwise. This reference uses the thermal electron convention. Thus, ion heats of formation are 1.48 kcal/mol larger than values that do not include the enthalpy of the electron. Uncertainties in parentheses. [b] Pedley, J. B.; Naylor, R. D.; Kirby, S. P. *Thermochemical Data of Organic Compounds*; Chapman and Hall: London, 1986. [c] Derived with $IP(CH_3) = 9.84 \pm 0.02$ eV (Houle, F. A.; Beauchamp, J. L. *J. Am. Chem. Soc.* **1979**, *101*, 4067). [d] Reference 45. [e] Szepes, L.; Baer, T. *J. Am. Chem. Soc.* **1984**, *106*, 273.

Table II. Heats of Formation (kcal/mol) at 298 K[a]

species	this work	literature
SiH	91.4 (1.8)	90.0 (2)[b]
SiH^+	273.6 (1.4)	273.8 (1.2)[c]
SiH_2^+		278.0 (1.4)[c]
SiH_3^+		237.5 (1.2)[c]
$SiCH^+$	339 (7)	
$SiCH_2^+$	290 (8), 285 (3)[d]	<355[e]
$SiCH_3^+$	231 (2), 235 (5)[f]	>269,[e] <289[e]
SiH_3C^{+*}	273 (4)	
$HSiCH_3^+$		244 (4)[g]
$H_2SiCH_2^+$		248 (4)[g]

[a] Thermal electron convention. The ion heats of formation are 1.48 kcal/mol larger than values that do not include the enthalpy of the electron. Uncertainties in parentheses. [b] Reference 34. [c] Reference 14. [d] Best value, taken from reaction 14 alone; see text. [e] Reference 8. [f] Average of all available experimental and theoretical values; see text. [g] Reference 32.

The second most probable reaction product is SiH^+ formed in reaction 5. (The heats of reaction for this and other processes

---

(16) Chesnavich, W. J.; Bowers, M. T. *J. Phys. Chem.* **1979**, *83*, 900.
(17) Elkind, J. L.; Armentrout, P. B. *J. Phys. Chem.* **1984**, *88*, 5454.
(18) Weber, M. E.; Armentrout, P. B. *J. Chem. Phys.* **1988**, *88*, 6898.
(19) Aristov, N.; Armentrout, P. B. *J. Am. Chem. Soc.* **1986**, *108*, 1806. Ervin, K. M.; Armentrout, P. B. *J. Chem. Phys.* **1986**, *84*, 6738. Sunderlin, L.; Aristov, N.; Armentrout, P. B. *J. Am. Chem. Soc.* **1987**, *109*, 78.
(20) Boo, B. H.; Armentrout, P. B. *J. Phys. Chem.* **1987**, *91*, 5777.
(21) Weber, M. E.; Elkind, J. L.; Armentrout, P. B. *J. Phys. Chem.* **1986**, *84*, 1521.

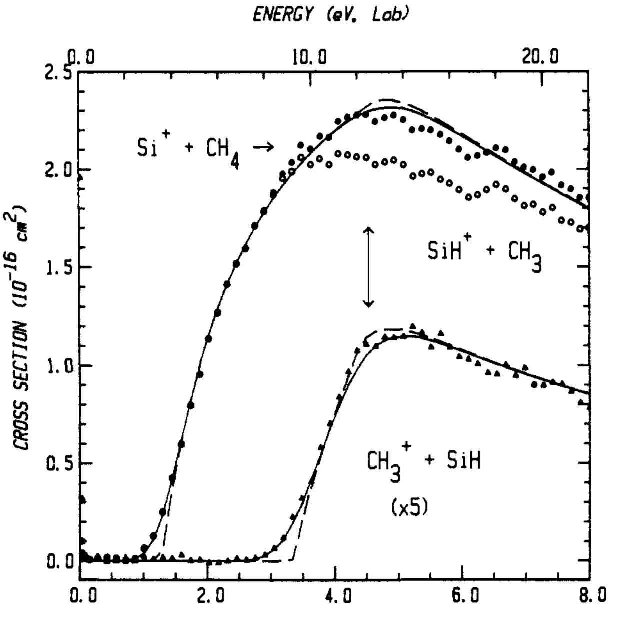

Figure 3. Cross sections for SiH^+ (open circles) and CH_3^+ (triangles) formed in the reactions of Si^+ with CH_4 as a function of the translational energy in the laboratory frame (upper scale) and the center-of-mass frame (lower scale). The sum of the two cross sections (closed circles) and the CH_3^+ data are compared with calculated cross sections as described in the text and Table III. The full lines show the models convoluted over the experimental energy distribution, and the broken lines show the unconvoluted fits. The arrow indicates $D^\circ(H-CH_3)$ at 4.54 eV.

discussed below are calculated from the literature thermochemistry given in Tables I and II.) The SiH^+ cross section rises rapidly

$$Si^+ + CH_4 \rightarrow SiH^+ + CH_3 - 1.28 \pm 0.07 \text{ eV} \qquad (5)$$

from near the expected threshold (Figures 1 and 3). The cross section is observed to reach a maximum around 4 eV and then declines slowly. Since the SiH^+ product can also decompose via reaction 4 beginning at 4.5 eV, this behavior suggests that the CH_3 product carries away considerable energy in either internal or translational modes. The contrasting behavior of the SiH_3C^+ product can then be attributed to the H atom product, which has no internal degrees of freedom and cannot carry away much energy in translation due to its light mass.

The cross section for SiH_2C^+ shown in Figures 1 and 4 exhibits two obvious features. These are explained by processes 6 and 7.

$$Si^+ + CH_4 \rightarrow SiH_2C^+ + H_2 \qquad (6)$$
$$\rightarrow SiH_2C^+ + H + H \qquad (7)$$

Note that the lower energy feature has an apparent threshold of about 0.6 eV, while the higher energy feature begins near 5 eV. The difference in the thresholds for reactions 6 and 7 correctly reflects the difference in endothermicities, 4.5 eV = $D^\circ(H_2)$. The SiH_2C^+ cross section falls off beginning about 7 eV. This could be due to product dissociation, processes 8 and 9. However, there

$$Si^+ + CH_4 \rightarrow SiHC^+ + H + H + H \qquad (8)$$
$$\rightarrow Si^+ + CH_2 + H + H - 9.3 \text{ eV} \qquad (9)$$

is not enough $SiHC^+$ product to account for the decline in the SiH_2C^+ cross section, and reaction 9 cannot occur until higher energies than the decline begins. We therefore attribute the decrease in this cross section to the loss of the precursor to the SiH_2C^+ product formed at high energies, namely SiH_3C^+. This species is rapidly lost via reaction 4. Thus, reaction 7 is a minor decomposition pathway for the SiH_3C^+ ion.

The small amount of $SiHC^+$ formed (Figure 1) must be due to reaction 10. This process has the latest onset among all observed product channels. It must be formed via H atom loss from SiH_2C^+ or via H_2 loss from SiH_3C^+.

$$Si^+ + CH_4 \rightarrow SiHC^+ + H_2 + H \qquad (10)$$

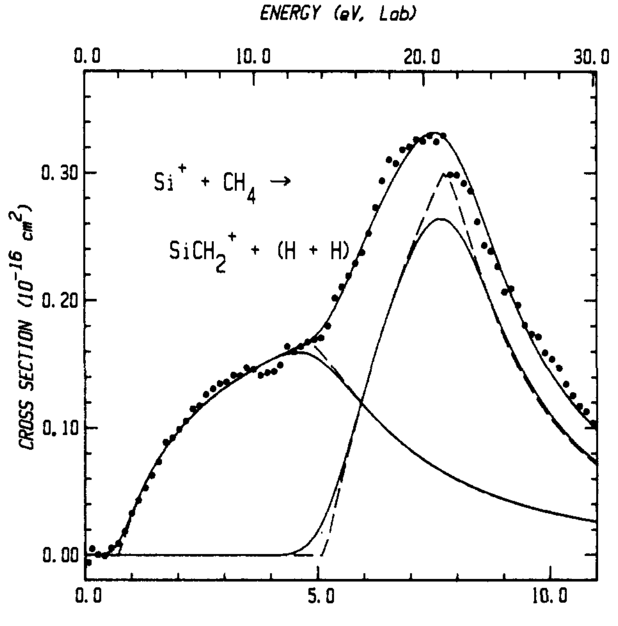

Figure 4. Cross section for $SiCH_2^+$ formed in the reactions of Si^+ with CH_4 as a function of the translational energy in the laboratory frame (upper scale) and the center-of-mass frame (lower scale). The experimental data (solid circles) are compared with calculated cross sections at low (reaction 6) and high (reaction 7) energies and their sum as described in the text and Table III. The full lines show the models convoluted over the experimental energy distribution, and the broken lines show the unconvoluted fits.

The final product observed is the methyl ion, a result of the hydride-transfer reaction, process 11. The apparent threshold (Figure 3) is in reasonable agreement with that calculated from Tables I and II. The cross section is observed to peak and then

$$Si^+ + CH_4 \rightarrow SiH + CH_3^+ - 3.21 \pm 0.10 \text{ eV} \qquad (11)$$

fall off beginning about 4.5 eV. This cannot be due to dissociation of CH_3^+ since fragmentation of this ion cannot occur until >8 eV. This means that the cross section declines due to competition with other reactions, most likely reaction 4.

Discussion

Structures. On the basis of the relative bond strengths of C–H and Si–H bonds, it seems reasonable to assume that the SiH_xC^+ species actually have the structures of $SiCH_x^+$. For $SiHC^+$, this is substantiated by recent theoretical calculations.[22] These indicate that both $SiCH^+$ and $HSiC^+$ isomers have a $^3\Sigma^-$ ground state but that linear $SiCH^+$ is more stable than $HSiC^+$ by 69 or 87 kcal/mol. These values are comparable to the stability difference of 61 kcal/mol predicted for the neutral counterparts.[22]

Similarly, Murrel, Kroto, and Guest have established that the isomerization of HSiCH to $SiCH_2$ is substantially exothermic and that the silylidene $:Si{=}CH_2$ is the absolute minimum on the potential energy hypersurface.[23] Further, Hopkinson and Lien found that this rearrangement occurs without a barrier.[24] Better quality calculations by Gordon and Pople confirm that $:Si{=}CH_2$ is more stable than silaethyne $HSi{\equiv}CH$ by 41 kcal/mol, but these authors find that a bent HSiCH structure is a local minimum on the potential energy surface.[25] In analogy with the $SiHC^+$ vs SiHC comparison, the lowest energy isomer for SiH_2C^+ is almost certainly $SiCH_2^+$.

---

(22) Bruna, P. S.; Hirsh, G.; Buenker, R. J.; Peyerimhoff, S. D. In *Molecular Ions*; Berkowitz, J., Groeneveld, K., Eds.; Plenum: New York, 1983; p 309.

(23) Murrel, J. N.; Kroto, H. W.; Guest, M. F. *J. Chem. Soc., Chem. Commun.* **1977**, 619.

(24) Hopkinson, A. C.; Lien, M. H. *J. Chem. Soc., Chem. Commun.* **1980**, 107.

(25) Gordon, M. S.; Pople, J. A. *J. Am. Chem. Soc.* **1981**, *103*, 2945.

Scheme I

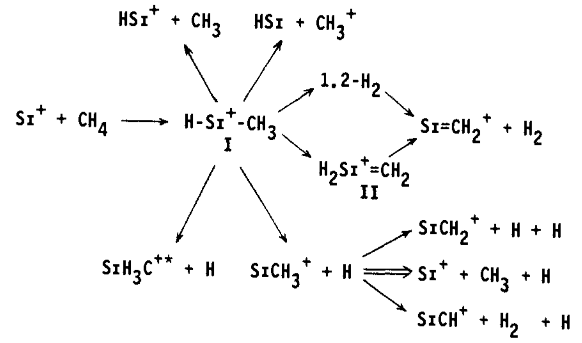

For the case of SiH_3C^+, Hopkinson and Lien[24] have calculated that $SiCH_3^+$ is the most stable isomer, followed by $HSiCH_2^+$ (57 kcal/mol higher in energy), H_2SiCH^+ (83 kcal/mol above $SiCH_3^+$), and H_3SiC^+ (139 kcal/mol above $SiCH_3^+$). They find that $HSiCH_2^+$ collapses without barrier into $SiCH_3^+$, although this conclusion can be questioned on the basis of the discussion of the SiH_2C isomers above. However, Ragavachari[26] also finds that $HSiCH_2^+$ in a singlet state rearranges without a barrier to the most stable $SiCH_3^+$ structure. He calculates that $HSiCH_2^+$ is 48 kcal/mol higher in energy and further finds that triplet states of $SiCH_3^+$ and $HSiCH_2^+$ lie 52 and 54 kcal/mol, respectively, above the singlet $SiCH_3^+$ ground state.

Reaction Mechanism. In the first stage of the reaction, silicon ion inserts into a C–H bond of methane to form $HSiCH_3^+$ (I) (Scheme I). This step is reasonable since the transient $HSiCH_3^+$ is more stable than $Si^+ + CH_4$ by 35 kcal/mol according to the thermochemical data of Tables I and II. Further, both experimental[17,27] and theoretical[22,28] results indicate that $Si^+(^2P)$ can insert into molecular hydrogen to form SiH_2^+. Since dihydrogen and methane have very similar bond strengths, it seems reasonable that $Si^+(^2P)$ can also insert into the C–H bond of methane to form I. Cleavage of the Si–C bond in I can then explain the formation of the observed $SiH^+ + CH_3$ and $SiH + CH_3^+$ products. Cleavage of the Si–H bond in I results in formation of ground-state $SiCH_3^+$, accounting for the low-energy feature in the SiH_3C^+ cross section. The high-energy feature in this cross section couuld be the result of H atom loss from the carbon to form $HSiCH_2^+$ in either a singlet or a triplet state or H atom loss from silicon to form $SiCH_3^+$ in a triplet state. Production of both singlet- and triplet-state products is spin-allowed, and as noted above, calculations[26] find that these three processes have nearly the same energetics. Further loss of an H atom from any of the SiH_3C^+ isomers or states can explain the high-energy source for the production of $SiCH_2^+$.

At low energies, formation of $SiCH_2^+$ could occur via two pathways, 1,2-dehydrogenation of I or, alternatively, rearrangement of I to $H_2SiCH_2^+$ (II) followed by 1,1-dehydrogenation from the silicon center. We note that the low-energy feature of the $SiCH_2^+$ cross section is smaller than that of the higher energy feature. This contrasts with the situation observed in the reactions of early-transition-metal ions with methane where the probability for forming $MCH_2^+ + H_2$ (M = Sc, Ti, V, Cr)[9] is much larger than that for the process leading to $MCH_2^+ + 2H$. In these systems, it is fairly clear that the structure of the MCH_2^+ species is a transition-metal carbene that is formed from $HMCH_3^+$ via 1,2-dehydrogenation. This four-center elimination is symmetry allowed because of the involvement of d electrons on the metal.[29] In the case of silicon, the inaccessibility of d electrons makes this process symmetry forbidden, explaining the inefficiency of this reaction channel. It is unknown whether this results in an overall barrier to the 1,2-dehydrogenation process, although Ragavachari has calculated that 1,2-dehydrogenation across $Si–Si^+$ bonds (the lowest energy dehydrogenation process) has a reverse activation barrier of about 7 kcal/mol.[30,31]

Table III. Values of n and E_0 Used To Model Excitation Functions[a]

system	product	n	E_0 (eV)
$Si^+ + CH_4$	$CH_3^+ + SiH$	1.0 (0.2)	3.27 (0.06)
	$SiH^+ + CH_3$	1.1 (0.1)	1.27 (0.06)
	$SiCH^+ + H_2 + H$	1.2	4.60 (0.10)
	$SiCH_2^+ + H_2$	1.2 (0.2)	0.72 (0.09)
	$SiCH_3^+ + H$	2.1 (0.2)	0.15 (0.06)
$Si^+ + C_2H_2$	$SiCH^+ + CH$	1.8 (0.2)	5.62 (0.04)
$Si^+ + C_2H_4$	$SiCH^+ + CH_3$	1.7 (0.1)	3.07 (0.06)
	$SiCH_2^+ + CH_2$	1.8 (0.2)	2.94 (0.11)
$Si^+ + C_2H_6$	$SiCH_3^+ + CH_3$		<0
$SiH^+ + CH_4$	$SiCH_3^+ + H_2$		<0

[a] Uncertainties in parentheses.

The alternate mechanism, rearrangement of I to II followed by 1,1-dehydrogenation, necessitates a hydrogen migration from carbon to silicon. In the neutral $HSi—CH_3$ to $H_2Si═CH_2$ rearrangement, the overall reaction is exothermic by 10 ± 3 kcal/mol,[32] but a sizable barrier to the H shift of 43 kcal/mol has been calculated theoretically.[7] In the similar rearrangement of the ionic counterpart, I to II, the barrier could be higher since the overall reaction is slightly endothermic, 4 ± 6 kcal/mol, and the $H_2Si^+═CH_2$ π bond being formed involves only one electron. Further, the similar hydrogen migration required to isomerize from $Si^+–CH_3$ to $HSi^+–CH_2$ has been calculated to require 48 kcal/mol,[26] as noted above. These considerations discount formation of II as a likely mechanism in the present system.

Thermochemistry. As discussed in the Experimental Section, the threshold for reaction can be determined with the use of eqs 1 and 2 to analyze the data. The parameters used in these analyses are given in Table III. The reaction thresholds are then combined with the literature thermochemistry listed in Table I to derive the thermochemical values in Table II. All reactants and products are assumed to be characterized by a temperature of 298 K, except for the kinetic energy of the reactant Si^+.

SiH^+. The cross section for the hydrogen atom transfer reaction 5 is reproduced by a line-of-centers model ($n = m = 1$ in eq 1). This analysis provides an endothermicity for the reaction of 1.28 ± 0.05 eV (average of 14 data sets). If n is allowed to optimize, we find $n = 1.07 \pm 0.09$ and $E_0 = 1.25 \pm 0.07$ eV. This form is shown in Figure 3, along with a high-energy fit where $p = 0$ and $E_D = 4.6$ eV $\approx D^\circ(H–CH_3)$. It can be seen that this reproduces the sum of the cross sections for reactions 5 and 11 very well.

When the average endothermicity of 1.27 ± 0.06 eV measured here is combined with the methane bond energy, $D^\circ(H–CH_3) = 4.54 \pm 0.01$ eV, this gives $D^\circ(Si^+–H) = 3.28 \pm 0.06$ eV. This value is in excellent agreement with the value previously measured from the reaction of $Si^+ + H_2$, 3.27 ± 0.04 eV,[17] and with spectroscopic values of 3.27 ± 0.03 and 3.24 ± 0.08 eV.[33]

SiH. A line-of-centers model also provides the best fit to the data for reaction 11 up to ≈4.5 eV (even after n is optimized). The threshold of the reaction is found to be $E_0 = 3.27 \pm 0.06$ eV (average of 12 data sets). Figure 3 shows this model along with a high-energy fit where $p = 0$ and $E_D = 4.6$ eV. This threshold leads to a heat of formation for SiH of 91.4 ± 1.8 kcal/mol, in good agreement with the 90.0 ± 2 kcal/mol value given in the JANAF tables.[34]

$SiCH^+$. The threshold of reaction 10 is determined to be 4.60 ± 0.10 eV with the use of the excitation function shown in Table

---

(26) Ragavachari, K. Personal communication.

(27) Elkind, J. L.; Armentrout, P. B. Unpublished work. Armentrout, P. B. In *Structure/Reactivity and Thermochemistry of Ions*; Ausloos, P., Lias, S. G., Eds.; D. Reidel: Dordrecht, 1987; p 97.

(28) Hirst, D. M.; Guest, M. F. *Mol. Phys.* **1986**, *59*, 141.

(29) Steigerwald, M. L.; Goddard, W. A. *J. Am. Chem. Soc.* **1984**, *106*, 308. Rappe, A. K. *Organometallics* **1987**, *6*, 354.

(30) Ragavachari, K. *J. Phys. Chem.* **1988**, *92*, 6284.

(31) Ragavachari, K. *J. Chem. Phys.* **1988**, *88*, 1688.

(32) Shin, S. K.; Irikura, K. K.; Beauchamp, J. L.; Goddard, W. A. *J. Am. Chem. Soc.* **1988**, *110*, 24.

(33) (a) Carlson, T. A.; Copley, J.; Duric, N.; Elander, N.; Erman, P.; Larsson, M.; Lyyra, M. *Astron. Astrophys.* **1980**, *83*, 238. (b) Douglas, A. E.; Lutz, B. L. *Can. J. Phys.* **1970**, *48*, 247.

(34) Chase, M. W.; Davies, C. A.; Downey, J. R.; Frurip, D. J.; McDonald, R. A.; Syverud, A. N. *J. Phys. Chem. Ref. Data* **1985**, *14*, Supplement No. 1.

III. This value leads to $\Delta_f H^\circ(SiCH^+) = 333 \pm 3$ kcal/mol, which is in line with heats of formation derived by measuring thresholds for processes 12 and 13. Analyses of these cross sections yield

$$Si^+ + C_2H_2 \rightarrow SiCH^+ + CH \qquad (12)$$

$$Si^+ + C_2H_4 \rightarrow SiCH^+ + CH_3 \qquad (13)$$

endothermicities of 5.62 ± 0.04 and 3.07 ± 0.06 eV, respectively. These values lead to $\Delta_f H^\circ(SiCH^+) = 339 \pm 5$ and 346 ± 2 kcal/mol, respectively. These three values average to 339 ± 7 kcal/mol (Table II).

$SiCH_2^+$. The thermochemistry of $SiCH_2^+$ is determined from the measured endothermicities of two reactions. For reaction 6, the analysis of the threshold region, 0–4 eV, is shown in Figure 4 and given in Table III. The 0.72-eV endothermicity yields a $\Delta_f H^\circ(SiCH_2^+)$ value of 296 ± 3 kcal/mol (average of 18 data sets). This value is slightly above that derived from analysis of reaction 14. This process is endothermic by 2.94 ± 0.11 eV, which

$$Si^+ + C_2H_4 \rightarrow SiCH_2^+ + CH_2 \qquad (14)$$

provides $\Delta_f H^\circ(SiCH_2^+) = 285 \pm 3$ kcal/mol. These two values average to $\Delta_f H^\circ(SiCH_2^+) = 290 \pm 8$ kcal/mol. However, since reaction 6 could have a small barrier in excess of the endothermicity, as discussed above, the lower heat of formation may be more correct. Both values are consistent with the upper limit of 355 kcal/mol reported by Stewart et al.[8]

The 290 kcal/mol heat of formation means that reaction 7 should begin at 5.0 ± 0.3 eV, consistent with the data. The data can be reproduced if we make plausible assumptions about the high-energy behavior of reaction 6. The model at low energy shown in Figure 4 is given by eq 2 with $p = 2$ and $E_D = 4.78$ eV $= D^\circ(CH_2\text{–}H_2)$, the threshold for $SiCH_2^+$ dissociation. At higher energies, Figure 4 shows a model where $n = m = 1$, $E_0 = 5.15$ eV, $p = 2$, and $E_D = 7.7$ eV (chosen to best fit the data). When these two models are summed, the total $SiCH_2^+$ cross section is reproduced nicely as shown in Figure 4. Note that this secondary threshold suggests that $\Delta_f H^\circ(SiCH_2^+) \approx 294$ kcal/mol, in good agreement with the value derived from the threshold for reaction 6.

$SiCH_3^+$. Since $SiCH_3^+$ is the more stable isomer for SiH_3C^+, this species must be responsible for reaction 3 at threshold. The endothermicity of reaction 3 is determined to be 0.15 ± 0.06 eV (average of 18 data sets) (Table III). This is in agreement with the work of Cheng et al.[12] who concluded that this reaction had a threshold below 0.4 eV, although they incorrectly attributed this reaction to excited-state Si^+. Our value for the threshold yields $\Delta_f H^\circ(SiCH_3^+) = 231 \pm 2$ kcal/mol, which is in accord with the observations that this ion is also formed in *exothermic* reactions of Si^+ with H_3SiCH_3,[35,36] SiH^+ with CH_4,[37,38] and Si^+ with C_2H_6.[37] These observations provide upper limits to the heat of formation of $SiCH_3^+$ of 242,[39] 256, and 242 kcal/mol, respectively. Furthermore, Ragavachari[30] and Gordon[40] have calculated that the reaction of Si^+ with H_3SiCH_3 is exothermic by 4 and 4.7 kcal/mol, respectively. These values suggest that $\Delta_f H^\circ(SiCH_3^+) = 238$ and 237 kcal/mol, respectively.[39]

Our value is also consistent with rough values derived from electron-impact appearance potential (AP) measurements. Hobrock and Kiser find that the AP of this ion is 12.4 ± 0.3 and 17.1 ± 0.4 eV from $HSi(CH_3)_3$ and $Si(CH_3)_4$, respectively.[41] By assuming that the neutral products are $CH_4 + CH_3$ and three CH_3, respectively, we obtain heats of formation for $SiCH_3^+$ of 232 ± 7 and 237 ± 9 kcal/mol. Bradshaw et al.[42] find that the AP of $SiCH_3^+ + H_2 + H$ from CH_3SiH_3 is 12.8 eV. Combined with $\Delta_f H^\circ(H_3SiCH_3)$ from Table I, this yields $\Delta_f H^\circ(SiCH_3^+) = 236$ kcal/mol. The average of all experimental and theoretical values is 235 ± 5 kcal/mol, and this is taken to be the best value available.

Previously, Stewart et al. reported lower and upper limits for this heat of formation of 269 and 289 kcal/mol.[8] The lower limit, which clearly disagrees with the present conclusions, comes from an observation that reaction 15 is endothermic. More recent work

$$CH_3^+ + SiH_4 \rightarrow SiCH_3^+ + 2H_2 \qquad (15)$$

by Cheng et al.[12] finds that this reaction is exothermic (as originally reported by Beggs and Lampe[43]), which indicates that the 269 kcal/mol value is an upper limit to $\Delta_f H^\circ(SiCH_3^+)$.

SiH_3C^{+*}. As mentioned above, the odd shape of the SiH_3C^+ cross section (Figures 1 and 2) suggests that two different forms of SiH_3C^+ are being produced, $SiCH_3^+$ at low energy and some excited state or isomer, SiH_3C^{+*}, at higher energies. A speculative interpretation of this cross section starts with the low-energy model for reaction 3 discussed above. To reproduce the shape near 2 eV, we then need to introduce competition with reaction 5 beginning at $E_D = 3.27$ eV ($p = 0$) and dissociation to $Si^+ + CH_3$, reaction 4, beginning at $E_D = 4.54$ eV ($p = 4$). This model is shown in Figure 2. The remainder of the SiH_3C^+ cross section can then be reproduced with $n = 1.3$, $m = 1.0$, $E_0 = 2.2$ eV, $p = 4$, and $E_D = 5.2$ eV. This high-energy model and its sum with the low-energy model are shown in Figure 2. (Note that, above 6 eV, this model reproduces the sum of the SiH_3C^+ and $SiCH_2^+$ cross sections. This is correct behavior since the models used incorporate only dissociation via reaction 4 and do not include reaction 7.) While speculative, this decomposition of the behavior of the SiH_3C^+ cross section is at least plausible and suggests that SiH_3C^{+*} has a heat of formation of ~278 kcal/mol.

A consistent value is obtained from results for reaction of SiH^+ with CH_4.[38] The cross section for the product channel of SiH_3C^+ is observed to have two distinct features, one exothermic channel and another endothermic one. The low-energy feature must correspond to formation of ground-state $SiCH_3^+$, while the high-energy feature is presumably due to SiH_3C^{+*}. The latter process is determined to be endothermic by 0.76 ± 0.1 eV, which provides a heat of formation for SiH_3C^{+*} of 273 ± 4 kcal/mol. The difference between this value and the $\Delta_f H^\circ(SiCH_3^+)$ value is 38 ± 6 kcal/mol. This is in fair agreement with theoretical values for the singlet state of $HSiCH_2^+$ and the triplet states of $SiCH_3^+$ and $HSiCH_2^+$, 48, 52, and 54 kcal/mol, respectively.[26]

Bond Energies. On the basis of $\Delta_f H^\circ(SiCH_3^+) = 235 \pm 5$ kcal/mol, the Si–C single-bond strength is 97 ± 5 kcal/mol. This is considerably larger than $D^\circ(Si^+\text{–}H) = 75.4 \pm 0.9$ kcal/mol. This difference can be observed directly in Figure 1 as the difference in thresholds for production of $SiCH_3^+ + H$ and $SiH^+ + CH_3$. These bond energies imply that the methyl radical can stabilize Si^+ more than atomic hydrogen can by 22 ± 5 kcal/mol. This seems to be a rather large stabilization energy but is comparable to $D^\circ(HSi^+\text{–}CH_3) - D^\circ(H_3CSi^+\text{–}H) = (65 \pm 4) - (39 \pm 5) = 26 \pm 6$ kcal/mol and to $D^\circ(HSi^+\text{–}CH_3) - D^\circ(HSi^+\text{–}H) = (65 \pm 4) - (48 \pm 2) = 17 \pm 5$ kcal/mol. We also note that the methyl stabilization energy becomes increasingly less as more ligands are placed on the silicon center. Thus, for SiX_3^+ and SiX_4^+ species (where X equals any combination of H and CH_3), the average stabilization energies for methyl substitution are 11 and 5 kcal/mol, respectively.[44] This trend is consistent with the observation that the methyl stabilization energy for neutral SiX_4 species is about zero.[45]

---

[35] Mandich, M. L.; Reents, W. D.; Bondybey, V. E. *J. Phys. Chem.* **1986**, *90*, 2315.

[36] Mayer, T. M.; Lampe, F. W. *J. Phys. Chem.* **1974**, *78*, 2422. These authors report that this reaction is endothermic, in direct contradiction to the results of ref 35. This study is complicated by the presence of excited-state Si^+ and secondary reactions.

[37] Boo, B. H.; Armentrout, P. B. Work in progress.

[38] This reaction has been previously reported in refs 8 and 12, although these results are not unambiguous due to the uncharacterized internal energy of the reactant ion.

[39] This value is derived using $\Delta_f H^\circ(SiH_3) = 48.5$ kcal/mol.[14]

[40] Gordon, M. S. Personal communication.

[41] Hobrock, B. G.; Kiser, R. W. *J. Phys. Chem.* **1961**, *65*, 2186; **1962**, *66*, 155.

[42] Bradshaw, D. I.; Moyes, R. B.; Wells, P. B. *Can. J. Chem.* **1976**, *54*, 599.

[43] Beggs, D. P.; Lampe, F. W. *J. Phys. Chem.* **1969**, *73*, 4194.

[44] The heats of formation needed for these numbers are calculated with the photoionization appearance potentials determined by R. R. Corderman and J. L. Beauchamp (Corderman, R. R. Ph.D. Thesis, Caltech, Pasadena, CA, 1977) and the neutral heats of formation given by Walsh.[45]

The Si^+–CH_2 and Si^+–CH bond energies are 104 ± 3 and 100 ± 7 kcal/mol, respectively. It is surprising that these bonds are no stronger than $D°(Si^+–CH_3)$, although this is certainly consistent with the notion that silicon does not readily make π bonds with carbon. One rationale for why no apparent π bond is formed in the $SiCH_2^+$ and $SiCH^+$ molecules is that Si^+ has a valence electron configuration of $3s^23p^1$. Thus, formation of a single bond to Si^+ can occur readily with the lone p electron, while formation of a double bond requires disruption of the fully occupied $3s^2$ orbital. This means that it may be more appropriate to compare $D°(Si^+–CH_2)$ and $D°(Si^+–CH)$ with $D°(HSi^+–CH_3)$ = 65 ± 4 kcal/mol. This comparison implies that π bonds of ~35 kcal/mol may be formed in these molecules. This is in reasonable agreement with the π bond energy in $H_2Si{=}CH_2$ of 34 ± 4 kcal/mol calculated by Shin et al.[32] and that in $H_3CSi{=}CH_2$ of 39 ± 5 kcal/mol estimated by Walsh.[45]

Acknowledgment. This work was supported by a grant from the National Science Foundation (Grant No. CHE-8917980) and by the Air Force Wright Aeronautical Laboratories. B.H.B. is grateful to the Korea Science and Engineering Foundation for partial financial support. We also thank K. Ragavachari and M. S. Gordon for communicating results prior to publication and to K. Ragavachari for helpful conversations.

---

(45) Walsh, R. *Acc. Chem. Res.* **1981**, *14*, 246.

AM1 Studies of E2 Reactions. 1. Mechanism and Leaving Group Effects

Michael J. S. Dewar* and Yate-Ching Yuan

Contribution from the Department of Chemistry, The University of Texas at Austin, Austin, Texas 78712.

Received August 10, 1989

Abstract: The mechanisms of bimolecular gas-phase elimination (E2) reactions have been studied, by use of the AM1 model. Calculations are carried out for E2 reactions between a base (B) and a molecule H-CHR-CHS-X, where B is methoxide anion and X is a neutral leaving group (Cl, Br, I, NO_2, $OCOCF_3$), and where B is a neutral base (ammonia) and X is an 'onium ion [$^+OH_2$, $^+OHCH_3$, $^+OC_2H_6$, $^+SH_2$, $^+SH(CH_3)$, $^+NH_3$]. The results are compared with experiment, and earlier calculations and interpretations.

Bimolecular base-induced elimination reactions, classed as E2 by Ingold,[1] represent one of the most important and most thoroughly documented classes of organic reactions. Here we will be concerned with the most common reactions of this kind, involving the 1,2-elimination of HX from adjacent carbon atoms of an organic compound; viz.

$$B + H{-}CHR{-}CHS{-}X \rightarrow BH^+ + RCH{=}CHS + X^- \quad (1)$$

where B is a base and R and S are substituents or hydrogen. Extensive mechanistic studies of such reactions have been reported, both in solution[2,3] and in the gas phase.[4-12]

Chart I. Variable Transition State of Elimination

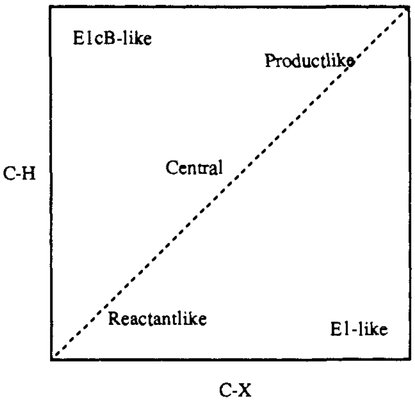

Reactions of this kind involve a combination of two basic processes; removal of a hydrogen atom β to X by the base, and ionization of C–X. These may take place in a single kinetic step (E2 mechanism) or in two distinct steps, the first step usually being rate determining. In an E1cB elimination, deprotonation occurs

---

(1) (a) Hanhart, W.; Ingold, C. K. *J. Chem. Soc.* **1927**, 997. (b) Hughes, E. D.; Ingold, C. K. *Trans. Faraday Soc.* **1941**, *37*, 657.

(2) Reviews: (a) Bartsch, R. A.; Zavada, J. *Chem. Rev.* **1980**, *80*, 453. (b) Cockerill, A. F.; Harrison, R. A. *The Chemistry of Double-Bonded Functional Groups*; Patai, S., Ed.; Wiley-Interscience: New York, 1977; Part I, pp 155–189. (c) Alekserov, M. A.; Yufit, S. S.; Kucherov, V. F. *Russ. Chem. Rev.* **1978**, *47*, 134. (d) Saunders, W. H., Jr.; Cockerill, A. F. *Mechanisms of Elimination Reactions*, Wiley: New York, 1973. (e) Ingold, C. K. *Structure and Mechanism in Organic Chemistry*, 2nd ed.; Cornell University Press: Ithaca, NY, 1969. (f) Saunders, W. H. *The Chemistry of Alkenes*, Patai, S., Ed.; Wiley: New York, 1964; p 149. (g) Hine, J. S. *Physical Organic Chemistry*; McGraw-Hill: New York, 1962; Chapters 7 and 8. (h) Gould, E. S. *Mechanism and Structure in Organic Chemistry*; Holt, Rinehart and Winston: New York, 1962; Chapter 12. (i) Bunton, C. A. *Reaction Mechanism in Organic Chemistry, Vol. 1, Nucleophilic Substitution at a Saturated Carbon Atom*; Hughes, E. D., Ed.; Elsevier Publishing Co.: London, 1963. (j) Banthorpe, D. V. *Reaction Mechanism in Organic Chemistry, Vol. 2, Elimination Reactions*; Hughes, E. D., Ed.; Elsevier Publishing Co.: London, 1963.

(3) (a) Baciocchi, E. *Acc. Chem. Res.* **1979**, *12*, 430. (b) Saunders, W. H., Jr. *Acc. Chem. Res.* **1976**, *9*, 19. (c) Bartsch, R. A. *Ibid.* **1975**, *8*, 239. (d) Fry, A. *Chem. Soc. Rev.* **1972**, *1*, 163. (e) Cordes, E. H.; Jencks, W. P. *J. Am. Chem. Soc.* **1963**, *85*, 2843. (f) Bourns, A. N.; Smith, P. J. *Can. J. Chem.* **1966**, *44*, 2553. (g) Cowell, G. W.; Ledwith, A.; Morris, D. G. *J. Chem. Soc. B* **1967**, 697. (h) Rosenthal, N. A.; Oster, G. *J. Am. Chem. Soc.* **1961**, *83*, 4445. (i) Wallace, T. J.; Hoffmann, J. E.; Schriesheim, A. *J. Am. Chem. Soc.* **1963**, *85*, 2739; **1964**, *86*, 1561.

(4) (a) Sullivan, S. A.; Beauchamp, J. L. *J. Am. Chem. Soc.* **1977**, *99*, 5017. (b) Sullivan, S. A.; Beauchamp, J. L. *Ibid.* **1976**, *98*, 1160. (c) Ridge, D. P.; Beauchamp, J. L. *Ibid.* **1974**, *96*, 637.

(5) van Doorn, R.; Jennings, K. R. *Org. Mass Spectrom.* **1981**, *16*, 397.

(6) DePuy, C. H.; Bierbaum, V. M. *J. Am. Chem. Soc.* **1981**, *103*, 5034.

(7) DePuy, C. H.; Beedle, E. C.; Bierbaum, V. M. *J. Am. Chem. Soc.* **1982**, *104*, 6483.

(8) Bierbaum, V. M.; Filley, J.; DePuy, C. H.; Jarrold, M. F.; Bowers, M. T. *J. Am. Chem. Soc.* **1985**, *107*, 2818.

(9) de Koning, L. J.; Nibbering, N. M. M. *J. Am. Chem. Soc.* **1987**, *109*, 1715.

(10) Werefridus, W.; van Berkel, L. J.; de Koning, J.; Nibbering, N. M. M. *J. Am. Chem. Soc.* **1987**, *109*, 7602.

(11) Jones, M. E.; Ellison, G. B. *J. Am. Chem. Soc.* **1989**, *111*, 1645.

(12) (a) Occhiucci, G.; Speranza, M.; de Koning, L. J.; Nibbering, N. M. M. *J. Am. Chem. Soc.* **1989**, *111*, 7387. (b) Angelini, G.; Lilla, G.; Speranza, M. *J. Am. Chem. Soc.* **1989**, *111*, 7393.

0002-7863/90/1512-2088$02.50/0